Applied Surface Science 56–58 (1992) 117–122
North-Holland

applied
surface science

Surface diffraction on semiconductor surfaces and interfaces

I.K. Robinson
AT&T Bell Labs, Murray Hill, NJ 07974, USA

Received 6 May 1991; accepted for publication 16 May 1991

Interface structures have relatively few general means available for their study. Surfaces, on the other hand, are widely accessible with electron-based techniques. X-ray diffraction has the important advantage of being sufficiently sensitive to detect a single layer of atoms, but at the same time being sufficiently penetrating to reach buried interfaces. It can therefore be used equally with surfaces and interfaces. The first half of this paper introduces the theoretical basis of the technique. Semiconductor surface and interface structures studied so far reveal the widespread importance of *strain fields*, often affecting several layers. Simple examples of this phenomenon are the Si(111) and Si(100) clean surface reconstructions, but the effects are just as important in adsorbate-induced structures, such as Pb/Si(111) or B/Si(111). Inclusion of the strain contributions to the free energy of these systems is *essential* for a theoretical understanding of why these structures are stable. Co_2Si/Si(111), Co_2Si/Si(100), and B-Si(111)/Si(111) interfaces also show some of the same effects.

1. Introduction

This paper discusses the application of X-ray diffraction to the study of surface and interface structures. The techniques described are already in limited use, but are likely to become more widespread in the future, particularly when based on a source of synchrotron radiation such as the European Synchrotron Radiation Facility (ESRF), presently under construction in Grenoble. In recognition of this potential, one of the first ten beamlines there is being dedicated entirely to surfaces and interfaces.

An interface is an internal surface, the boundary between two media that may be crystalline, amorphous solid or liquid. Its close similarity with a surface, a solid–vacuum boundary, means that the two problems may be handled analogously from the point of view of X-ray diffraction. Traditional, electron-based surface methods were developed to be non-penetrating in order to have surface sensitivity. This works against us in the interface situation by requiring the use of extremely thin samples, on one side of the interface, at least. This means special handling of samples in some cases and raises the possibility of artifactual results. Of the various methods, X-ray diffraction is the most penetrating and least surface sensitive; it probably has the greatest potential for widespread use in interface science.

We will define *structure* as atomic structure for this purpose: we are interested in the coordinates of atoms at the interface and their relation to bulk structures on one or both sides. For this reason we will consider only interfaces which are crystalline on at least one side. Since crystals are by far our strongest structural reference point, much less can be said about other interfaces. We will also consider the *morphology* of an interface, defined as the boundary of the crystal(s) that demarcates the interface, also at the atomic level. This is most apparent in the form of interface roughness. The roles of strain and misfit dislocations in interface formation, also studied by these techniques, are important too.

2. X-ray diffraction

The basic principles of X-ray diffraction from interfaces are even simpler than for electron

diffraction because the kinematic approximation is generally applicable. For X-ray wavelengths of order 1 Å and relatively light materials the penetration is limited by photoelectric absorption to a depth of microns, provided the grazing angle regime is avoided. Thus, to a reasonable approximation for interfaces within about 1000 Å of an accessible surface, there is no penetration problem, and the diffraction from an interface can be seen superimposed on that of the bulk surrounding it. Needless to say, that bulk contribution is far from negligible as it arises from a far greater amount of material.

Fig. 1 shows a schematic picture of the differences and similarities between surfaces and interfaces. Fig. 2 shows the Fourier transform of fig. 1, representing the situation in reciprocal space. An ideal, floating 2D layer has diffraction in the form of continuous lattice rods of constant intensity (ignoring vibration and the finite size of the atoms). If this layer is the surface layer of a crystal, or an interfacial layer, it has the same periodicity as the bulk of the crystal; the lattice

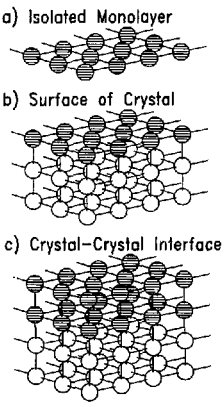

Fig. 1. Ball and stick models of crystal lattices for consideration of surface and interface diffraction.

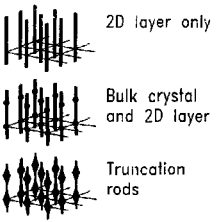

Fig. 2. Diagrammatic diffraction patterns of the objects in fig. 1.

rods then pass through the discrete Bragg reflections of the bulk. The general construction of the diffraction of a terminated crystal, or one with an internal interface includes the *interference* between these, as shown at the bottom of fig. 2: here there is a smooth crossover from surface to bulk diffraction. The lattice rods have the characteristic shape of *crystal truncation rods* [1]. CTRs are the X-ray equivalent of the continuous rods seen in low-energy electron diffraction (LEED), but have orders of magnitude more modulation because the penetration is so much greater.

The sensitivity of crystal truncation rods (CTRs) to interface structure and morphology is shown in fig. 3. Superimposed are calculated curves for an ideally terminated surface, a surface that is rough in the statistical sense of having random atoms omitted in one layer, and a surface with a modification of the spacing. In the vicinity of the divergences of the function (the Bragg points) all curves converge: here there is *no* structural sensitivity. Elsewhere, and notably at the mid-point of the CTR, there is *considerable* structural sensitivity.

The advantage of X-rays, particularly those produced by electron storage rings at facilities like the ESRF, is their very high resolution. The typical resolution function of a 3-axis diffractometer fills only 5×10^{-10} of the Brillouin zone of Si. The bulk diffraction is localized in point-like bragg peaks, smaller than this resolution element. Point defects and bulk thermal diffuse scattering (TDS) are diffuse in all reciprocal space direc-

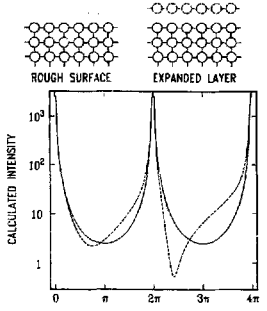

Fig. 3. Calculated crystal truncation rod profiles for an ideal terminated surface (solid curve), compared with rough and modified surfaces. The curves diverge at bulk Bragg points.

tions. As figs. 1 and 2 illustrate, the virtue of their 2-dimensional translational symmetry gives rise to rod-like lines of scattering; everything else can be filtered out either by avoidance (3D Bragg peaks) or else by background subtraction (diffuse scattering). Distinguishing the buried interface from the surface through which it is measured is then the only outstanding problem.

3. SiO_2/Si(111) interface

The overall situation is not quite the same for the crystal/amorphous and the crystal/crystal interface, so we will consider an example of each. For a direct comparison with previous work [2] carried out by LEED, we show X-ray diffraction intensity data for the Si(111)/SiO_2 interface [3] in fig. 4. The data shown are filtered in the manner described above, so correspond to diffraction from this interface alone. Since the SiO_2 film is amorphous there is no crystalline contribution to the CTR from the external surface either. The dashed curve is the calculated crystal truncation rod [1] of a Si crystal terminating with an ideal Si(111) bilayer. As stated above, midway between the Bragg peaks, alternate layers scatter out of phase and the observation is most sensitive to steps. This is where we see the largest deviations in fig. 4. The solid curve includes an atomic model of the interface that adds three half bilayers of Si with partial occupancy [3] and leads to an extremely good fit. The RMS height deviation of this model [3] is 1.53 Å, in excellent agreement with LEED [2]. No information was obtained about the *lateral* distribution of the steps.

Other X-ray measurements of the Si(111)/SiO_2 interface have been made. Cowley and Ryan

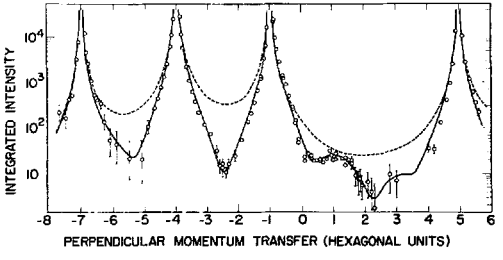

Fig. 4. X-ray measurement of the first-order crystal truncation rod (CTR) of the Si(111)/SiO_2 interface. Each point is the integrated intensity of a rocking scan with the diffuse background subtracted. Four bulk peaks are intersected where the CTR diverges, as in fig. 3.

[4] measured the zero-order CTR on the side of the (111) Bragg peak for a variety of different thin oxides. They found almost ideal $|q|^{-2}$ dependence of the intensity in all cases, using data spanning momentum transfer deviations, $|q|$, up to 0.4 in the units of fig. 1. This implies an RMS roughness of 0 ± 2 Å, which is within error of the values obtained above [2,3]. According to fig. 4, the slightly rough surface (solid curve) does deviate from the ideal (dashed) noticeably by $|q| = 0.4$, but this is asymmetric about the Bragg peaks because of a slight contraction within each of the Si(111) bilayers [3]. An asymmetry has also been detected by Harada and Kashiwagura [5] in similar measurements of CTRs from the Si(111)/SiO_2 interface.

4. $NiSi_2$/Si(111) interface

We turn now to our second example, the Si(111)/$NiSi_2$ interface, shown schematically in fig. 5. The lattice mismatch between Si and $NiSi_2$ is extremely small, 0.005 at room temperature and smaller still at the elevated temperatures of its growth. When a sufficiently thin film of $NiSi_2$ is grown on Si, it undergoes a slight hexagonal distortion so that the in-plane parameters match exactly. The critical film thickness, below which the distortion takes place, is many hundreds of ångströms. The figure shows the known B-type atomic arrangement of the interface with its reversal of stacking sequence (see below) and coordination number 7 at the Ni. Other configurations might be constructed, for example with one less layer of Si and the interfacial bonds linking directly to the Ni. These ultimately result in a different value of the parameter d, which is the fundamental structural parameter. A complete description of the structure would also include the strain fields on each side, that might extend several layers deep.

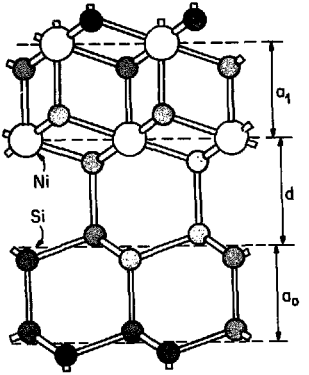

Fig. 5. Schematic model of the B-type Si(111)/$NiSi_2$ interface. If all the bonds were of ideal length, the interfacial separation parameter, d, would be 9/8 times the layer spacing, a_0.

Diffraction from a crystal/crystal interface is necessarily different because *both* crystals contribute: there is a CTR from the thick (i.e., semi-infinite) substrate and a finite-size-limited Bragg peak from the thin film, which is also a streak of continuous scattering diffuse in the direction perpendicular to the film. Since the *lateral* lattice parameters are matched, these rods superimpose. Since the film is adjacent to the substrate, the diffraction amplitudes must interfere in a way that is critically dependent upon the separation, which is our structural parameter d. Other details are important too: the choice of termination at each side, the strain fields, the lateral registry, the roughness of the outer surface, etc. Analysis of the intensity along the rod can determine all of these, in principle.

The measured intensity [6] along the rod in the vicinity of the (111) Bragg peak is shown in fig. 6. The peak is clearly asymmetric about the divergence at the Bragg position. The respective contributions of the substrate CTR and the thin film are drawn as labelled, dashed curves. The number of layers was determined by the node spacing to be an admixture of 7 and 8. These curves are individually symmetric about their centers, but the amplitude superposition yields a strong asymmetry. The first reason for this is that d is greater than the lattice spacing; second, a_1 is slightly

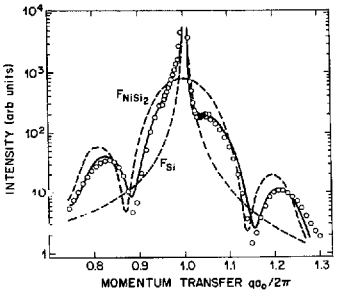

Fig. 6. X-ray diffraction intensity profile of the rod passing through the Si(111) Bragg peak of the Si(111)/$NiSi_2$ interface. (Adapted from ref. [6].)

smaller than a_0, leading to a slight difference in the center positions. The combined fit shown leads to an accurate determination [6] of both d and $a_{\parallel}$. The interface is contracted by 0.08 ± 0.06 Å from the configuration of ideal bondlengths (which would give $d = 9/8$). The roughness of the outer surface was found to be negligible for this particular sample.

Van Loenen et al. [7] used medium-energy ion scattering, not only to prove the 7-fold coordination model of fig. 3, but also to determine the parameter d to some accuracy. The value obtained corresponds to a contraction of the interface with respect to the ideal geometry of 0.06 ± 0.08 Å, comparing favorably with the later X-ray measurement [6]. The most accurate determination of d comes from the X-ray standing wave technique, giving contractions of 0.11 ± 0.03 Å [8] and 0.06 ± 0.03 Å [9] for the two experiments on films of very different thickness.

5. Boron at Si(111) interfaces

Boron deposition on the Si(111) surface is found to induce a $\sqrt{3} \times \sqrt{3}$ reconstruction, just as various metals are found to do. This can also be obtained by segregation from a B-doped wafer. Analysis of the metal induced structures by X-ray diffraction and other techniques revealed the so-called T4 adatom structure, shown for Ga/Si(111) on the left of fig. 7. This represents the structure

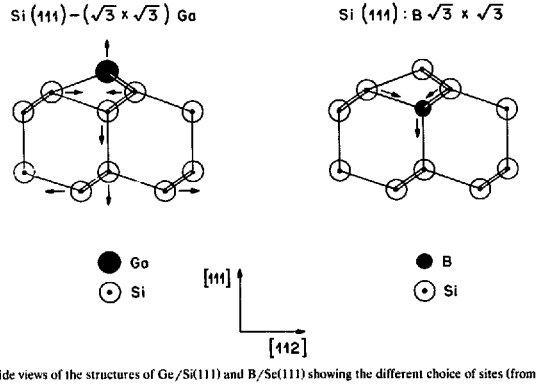

Fig. 7. Side views of the structures of Ge/Si(111) and B/Si(111) showing the different choice of sites (from ref. [14]).

of Sn/Si(111) [10], Pb/Ge(111) [11], Bi/Si(111) [12] and Sn/Ge(111) [13] all at low coverage ($\frac{1}{3}$ monolayer). In each case, the induced strain leads to inward contraction of the immediate Si neighbours of the adatom. This results in perpendicular displacements in layers 2 and 3 (see fig. 7) and consequently to *outward* relaxation of the three 4th-nearest neighbours in the 4th layer. The magnitudes and signs of these lateral components are found to be very similar. The accuracy of the lateral components is always much better than for the perpendicular components because of the far greater range of in-plane than out-of-plane momentum transfer in the typical surface X-ray experiment. The fits to rod-scan data for Sn/Ge(111) and Pb/Ge(111) show dramatic intensity modulations arising from the multilayer nature of the reconstruction [11,13].

A striking exception is the B/Si(111) structure, also drawn in fig. 7, for which the 4th layer displacement is in the *opposite* sense and considerably smaller [14]. This situation arises because the B atom occupies an altogether different site, the substitutional S5 site. Since the B–Si bondlength is around 15% shorter than Si–Si, this site is accommodated with less resulting strain than the T4 site. It consequently explains why a single layer of B can be largely retained at low temperature in an a-Si/Si interface, while this situation in untenable with Ga for example [15].

This unexpected S5 site for B/Si(111) results in very different behaviour of this $\sqrt{3} \times \sqrt{3}$ surface towards subsequent overgrowth of Si [16]. Since boron starts to diffuse at temperatures below the necessary growth temperatures of *crystalline* Si on Si, the experiment is performed in two stages. First a deposition of a-Si on B/Si(111) $\sqrt{3} \times \sqrt{3}$ is made at 400 °C, which gives rise to relatively little B segregation [16]. This is followed by a post-anneal at 540 °C, leading to overgrowth. The resulting Si crystal has the type-B interface containing a stacking fault. The designation "B" (as opposed to "A") was made long before the role of boron was discovered! Since the boron would have diffused away at the regrowth temperature, the choice of orientation must be induced at the a-Si template stage [15], and probably is due to more efficient relief of strain in the locally faulted structure, although chemical-bonding arguments could also be invoked [16].

Acknowledgements

Many people have contributed to the general ideas represented in this paper and the experimental results displayed: J. Bohr, J.D. Axe, M. Nielsen, R. Feidenhans'l, R.T. Tung, W.K. Waskiewicz, E. Vlieg, R.L. Headrick and L.C. Feldman. Experiments were carried out at the Stanford Synchrotron Radiation Laboratory, which is supported by US DoE and NIH programs, and at the National Synchrotron Light Source which is supported by the US DoE under grant DE-AC012-76CH00016.

References

[1] I.K. Robinson, Phys. Rev. B 33 (1986) 3830.
[2] J. Wollschläger and M. Henzler, Phys. Rev. B 39 (1989) 6052.
[3] I.K. Robinson, W.K. Waskiewicz, R. Tung and J. Bohr, Phys. Rev. Lett. 57 (1986) 2714.
[4] R.A. Cowley and T. Ryan, J. Phys. D 20 (1987) 61.
[5] J. Harada and N. Kashiwagura, J. Phys. (Paris) 50 (1989) C7-129.
[6] I.K. Robinson, R.T. Tung and R. Feidenhans'l, Phys. Rev. B 38 (1988) 3632.
[7] E.J. van Loenen, J.W.M. Frenken, J.F. van der Veen and S. Valeri, Phys. Rev. Lett. 54 (1985) 827.
[8] E. Vlieg, A.E.M.J. Fischer, J.F. van der Veen, B.N. Dev and G. Materlik, Surf. Sci. 178 (1986) 36.
[9] J. Zegenhagen, K.G. Huang, W.M. Gibson, B.D. Hunt and L.J. Schowalter, Phys. Rev. Rev. B 39 (1989) 254.
[10] K.M. Conway, J.E. Macdonald, C. Norris, E. Vlieg and J.F. van der Veen, Surf. Sci., to be published.
[11] R. Feidenhans'l, J.S. Pedersen, M. Nielsen, F. Grey and R.L. Johnson, Surf. Sci. 178 (1986) 927.
[12] T. Takahashi, I. Takayama, T. Ishikawa, T. Ohta and S. Kikuta, Jpn. J. Appl. Phys. 24 (1985) L727;
T. Takahashi, S. Nakatani, I. Ishikawa and S. Kikuta, Surf. Sci. 191 (1987) L825.
[13] J.S. Pedersen, R. Feidenhans'l, M. Nielsen, K. Kjær and R.L. Johnson, Surf. Sci. 189/190 (1987) 1047.
[14] R.L. Headrick, I.K. Robinson, E. Vlieg and L.C. Feldman, Phys. Rev. Lett. 63 (1989) 1253.
[15] R.L. Headrick, L.C. Feldman and I.K. Robinson, Appl. Phys. Lett. 55 (1989) 442.
[16] R.L. Headrick, B.E. Wier, J. Bevk, B.S. Freer, D.J. Eaglesham and L.C. Feldman, Phys. Rev. Lett. 65 (1990) 1128.